Received: 3 March 2022 | Accepted: 30 March 2022

DOI: 10.1002/mma.8296

RESEARCH ARTICLE

WILEY

Dynamic transitions and Turing patterns of the Brusselator model

Umar Faruk Muntari | **Taylan Şengül**

Department of Mathematics, Marmara University, Istanbul, Turkey

Correspondence
Umar Faruk Muntari, Department of Mathematics, Marmara University, Baglarbasi Mahallesi, Turgut Reis Street, No. 24, Istanbul 34722, Turkey.
Email: umarfaruk19@marun.edu.tr

Communicated by: M. Efendiev

The dynamic transitions of the Brusselator model has been recently analyzed in Choi et al. (2021) and Ma and Wang (2011). Our aim in this paper is to address the relation between the pattern formation and dynamic transition results left open in those papers. We consider the problem in the setting of a 2D rectangular box where an instability of the homogeneous steady state occurs due to the perturbations in the direction of several modes becoming critical simultaneously. Our main results are twofold: (1) a rigorous characterization of the types and structure of the dynamic transitions of the model from basic homogeneous states and (2) the relation between the dynamic transitions and the pattern formations. We observe that the Brusselator model exhibits different transition types and patterns depending on the nonlinear interactions of the pattern of the critical modes.

MSC CLASSIFICATION

37Lxx; 37Nxx

1 | INTRODUCTION

Dynamic transitions have been shown to occur in many branches of the nonlinear science.[1] Some recent examples include the thermohaline circulation,[2] chemotatic systems,[3] vegetation formation,[4] gas dynamics,[5] and quasi geostrophic flows.[6,7] One of the jewels of the nonlinear science has been the Brusselator and related chemical reaction models which have received extensive interest.[8–10] In this paper, we identify and classify transitions of Turing patterns for the Brusselator model which was introduced initially in Prigogine and Lefever.[11] The model displays some important aspects of the dynamical systems theory such as multistability[12] and irreversibility.[13] Our main paradigm is the dynamic transition theory originally introduced in Ma et al.[1]

As an example of Belousov–Zhabotinsky reaction, the mechanism of the Brusselator model is based on autocatalytic, oscillating chemical reaction. An autocatlytic reaction is one in which a species acts to increase the rate of its producing reaction. In many autocatlytic systems, multiple steady states and periodic orbits are usually seen.[14] The chemical reaction of the Brusselator model consists of four irreversible steps, given by

$$\begin{aligned} A &\xrightarrow{k_1} X \\ B + X &\xrightarrow{k_2} Y + D \\ 2X + Y &\xrightarrow{k_3} 3X \\ X &\xrightarrow{k_4} E \end{aligned} \tag{1}$$

where X and Y are components which vary in time and space, A and B are constant components while D and E are products.

Turing patterns are natural patterns which arise spontaneously in a number of natural phenomena such as animal coatings, chemical reactions, and patterns of sand dunes and vegetation patterns in ecology. The formations of these patterns are described by reaction–diffusion equations. A diffusion-driven instability also called the Turing instability occurs in a reaction–diffusion system when a homogeneous steady state is stable to small perturbation in the absence of diffusion but becomes unstable to small spatial perturbations when there is diffusion.[15] Mathematically, these equations possess a stable homogeneous equilibrium which will lose its stability as a control parameter exceeds some critical threshold. As this basic state loses stability, the system will move towards a new stable state, often displaying pattern structure which is known as Turing patterns.

In this article, we address the dynamic transition of Turing patterns of the Brusselator model by deriving a complete characterization of the transition from the homogeneous state. Our guiding principle is the dynamic transition theory of Ma et al.[1] The key philosophy of dynamic transition theory is to search for the full set of transition states, giving a complete characterization of stability and transition. The set of transition states is a local attractor, representing the physical reality after the transition. As a general principle, dynamic transitions of all dissipative systems are classified into three categories: continuous (Type-I), catastrophic (Type-II), and random (Type-III).[1,16] In more mathematical intuitive terms, the types are, respectively, called continuous, jump, and mixed. In the Brusselator model, the signs of some nondimensional computable parameters determine the transition types.

There have been two recent papers[8,17] which also dealt with the dynamic transitions of the Brusselator problem in different settings and with a different perspective. In Ma and Wang,[8] the emphasis is solely on the dynamic transitions and not on the pattern formations. More recently in Choi et al,[17] the problem is investigated in a one spatial variable setting. Although such simplifications are sometimes necessary to understand the basic mechanisms, to establish the relation between the pattern formations and dynamic transitions, at least two spatial variables are necessary which is the case studied in our paper. Thus, the goal of the current paper is to address the shortcomings of these two papers.

The organization of this paper is as follows. Section 2 deals with the mathematical model, and Section 3 focuses on the linear stability analysis and the principle of exchange of stabilities (PES). The main theorems and the dynamic transitions of the model are addressed in Section 4, while the proofs of the theorems are discussed in Section 5 with the conclusion in Section 6.

2 | THE MODEL AND ITS MATHEMATICAL SETUP

In this section, we present the mathematical representation of the Brusselator model together with the boundary conditions considered and then subsequently put it into an abstract functional setting. The classical Brusselator model of Prigogine and Lefever which in the nondimensionalized form reads

$$\begin{aligned} \partial_t u &= a - (b+1)u + u^2 v + d\Delta u \\ \partial_t v &= bu - u^2 v + \Delta v \end{aligned} \tag{2}$$

$a, b, d > 0$. We assume the Neuman boundary conditions on a 2D rectangular box.

$$\frac{\partial \mathbf{u}}{\partial n} = 0, \ \mathbf{u} = (u, v) \qquad \text{on } \partial\Omega, \ \Omega = (0, L\pi) \times (0, \pi) \tag{3}$$

where n is the outer normal of the domain Ω.

Equation 2 admits the constant solution.

$$(u_s, v_s) = (a, b/a)$$

The equations for the perturbations

$$\begin{pmatrix} u' \\ v' \end{pmatrix} = \begin{pmatrix} u \\ v \end{pmatrix} - \begin{pmatrix} u_s \\ v_s \end{pmatrix} \tag{4}$$

around this constant solution are as follows.

$$\partial_t \begin{pmatrix} u' \\ v' \end{pmatrix} = \begin{bmatrix} (b-1)+d\Delta & a^2 \\ -b & -a^2+\Delta \end{bmatrix} \begin{pmatrix} u' \\ v' \end{pmatrix} + \begin{bmatrix} \frac{b}{a}u'^2 + 2au'v' + u'^2v' \\ -\frac{b}{a}u'^2 - 2au'v' - u'^2v' \end{bmatrix} \tag{5}$$

We write (5) in the standard form by first defining the function spaces.

$$H = L^2(\Omega, \mathbb{R}^2) \tag{6}$$

$$H_1 = \left\{ \begin{pmatrix} u \\ v \end{pmatrix} \in H^2(\Omega, \mathbb{R}^2) : \frac{\partial u}{\partial n} = \frac{\partial v}{\partial n} = 0 \text{ on } \partial\Omega \right\} \cap H, \tag{7}$$

$$H_{1/2} = \left\{ \begin{pmatrix} u \\ v \end{pmatrix} \in H^1(\Omega, \mathbb{R}^2) : \frac{\partial u}{\partial n} = \frac{\partial v}{\partial n} = 0 \text{ on } \partial\Omega \right\} \cap H, \tag{8}$$

We also define the operators $L_b : H_1 \mapsto H$ and $G : H_{1/2} \mapsto H$ by

$$L_b\mathbf{u} = ((b-1)u + a^2v + d\Delta u, -bu - a^2v + \Delta v), \tag{9}$$

$$G(\mathbf{u}) = \left(\frac{b}{a}u^2 + 2auv + u^2v, -\frac{b}{a}u^2 - 2auv - u^2v \right) \tag{10}$$

Thus, (5) can be written as

$$\frac{d\mathbf{u}}{dt} = L_b\mathbf{u} + G(\mathbf{u}). \tag{11}$$

3 | LINEAR STABILITY ANALYSIS

In this section, we analyze the linear stability of the basic steady state of the model. Then we formulate this analysis as PES; see Theorem 1.

For this purpose, we start with defining the index set

$$\mathcal{K} = (k_1, k_2) \in \mathbb{Z}^2_{\geq 0}, \tag{12}$$

the wavenumber

$$k^2 = \frac{k_1^2}{L^2} + k_2^2, \qquad k \in \mathcal{K},$$

and the **modes**

$$e_{k_1,k_2}(x, y) = \cos\frac{k_1}{L}x \cos k_2 y, \qquad (k_1, k_2) \in \mathcal{K}.$$

The mode is said to have a **rectangular pattern** if $k_1 \neq 0$, $k_2 \neq 0$ and a **roll pattern** if either $k_1 = 0$ or $k_2 = 0$. The particular case $k_1 = k_2 \neq 0$ of a rectangular pattern is called a **square pattern**.

For $k = (k_1, k_2) \in \mathcal{K}$, plugging the ansatz

$$\begin{bmatrix} u_k \\ v_k \end{bmatrix} e_{k_1,k_2}(x, y) \tag{13}$$

into the eigenvalue problem

$$L_b e_k = \beta_k e_k, \tag{14}$$

yields the eigenvalue relation

$$\beta_k \begin{bmatrix} u_k \\ v_k \end{bmatrix} = A \begin{bmatrix} u_k \\ v_k \end{bmatrix} - k^2 D \begin{bmatrix} u_k \\ v_k \end{bmatrix} \tag{15}$$

where the operators A and D stand for

$$A = \begin{bmatrix} b-1 & a^2 \\ -b & -a^2 \end{bmatrix}, \qquad D = \begin{bmatrix} d & 0 \\ 0 & 1 \end{bmatrix}.$$

We can easily show that the eigenvectors are given by

$$\begin{bmatrix} u_k \\ v_k \end{bmatrix} = \begin{bmatrix} 1 \\ \frac{-b}{\beta_k + a^2 + k^2} \end{bmatrix} \tag{16}$$

and the eigenvalues satisfy

$$\det(\beta_k I - (A - k^2 D)) = \beta_k^2 - \tau_k \beta_k + \Delta_k = 0 \tag{17}$$

where

$$\tau_k = \mathrm{tr}(A - k^2 D) = b - 1 - a^2 - (d+1)k^2 \tag{18}$$

and

$$\Delta_k = \det(A - k^2 D) = a^2 + (a^2 d + 1 - b)k^2 + dk^4. \tag{19}$$

Hence, the eigenvalues are

$$\beta_k = \frac{\tau_k \pm \sqrt{\tau_k^2 - 4\Delta_k}}{2}. \tag{20}$$

Turing instability is defined as the stability of the equilibrium without diffusion, that is, $k = 0$ case, while instability with diffusion for some $k \neq 0$. This was the original idea of Turing which was a novel one since diffusion is often a stabilizing mechanism.

Since $\Delta_0 = \det(A) = a^2 > 0$, the stability of the equilibrium without diffusion only requires

$$\tau_0 = \mathrm{tr}(A) = b - 1 - a^2 < 0 \tag{21}$$

From (17), the instability in the presence of diffusion means that for some $k \neq 0$, exactly one of the following conditions (22) and (23) holds:

$$\Delta_k < 0 \tag{22}$$

or

$$\Delta_k > 0 \ \text{ and } \ \tau_k > 0. \tag{23}$$

Since $\tau_k \leq \tau_0$, $\tau_0 < 0$ implies that $\tau_k < 0$ for any k, (21) and (23) are incompatible. Thus for the Turing instability, one requires the following two conditions to hold.

$$\tau_0 < 0, \ \text{ and } \ \Delta_k < 0 \ \text{ for some } \ k \in \mathcal{K}. \tag{24}$$

The **critical Turing wavenumber** $k_T \in \mathcal{K}$ is determined as

$$k_T = \mathrm{argmin}_{k \in \mathcal{K}} \Delta_k. \tag{25}$$

To obtain k_T, we first consider the problem

$$0 = \frac{d}{dk^2}\Delta_k = \frac{d}{dk^2}\det(A - k^2 D) = \mathrm{tr}(D^{-1}A - k^2 I), \qquad k^2 \in \mathbb{R}^+ \tag{26}$$

whose solution is

$$\tilde{k}^2 = \frac{1}{2}\mathrm{tr}(D^{-1}A) = \frac{b - 1 - a^2 d}{2d}. \tag{27}$$

The **critical transition number** b_T is now determined by solving b from the relation

$$0 = \Delta_{\tilde{k}} = -\frac{(b-1)^2 - 2a^2(1+b) + a^4 d^2}{4d}$$

and is obtained as

$$b = \left(a\sqrt{d} \pm 1\right)^2.$$

However, only $b = \left(a\sqrt{d} + 1\right)^2$ in (27) gives a positive $\tilde{k}^2$. Thus, we define

$$b_T = \left(a\sqrt{d} + 1\right)^2.$$

Suppose that for $k_1, k_2 \in K$,

$$k_1^2 \le \tilde{k}^2|_{b=b_T} = \frac{a}{\sqrt{d}} \le k_2^2.$$

Then we define $k_T \in \mathcal{K}$ as

$$k_T^2 = \mathrm{argmin}_{k \in \{k_1, k_2\}} \Delta_k. \tag{28}$$

Since

$$\frac{d\Delta_k}{db} = -k^2 < 0,$$

the following transversality condition is satisfied

$$\Delta_{k_T} \begin{cases} > 0 & b < b_T \\ = 0 & b = b_T \\ < 0 & b > b_T \end{cases} \tag{29}$$

which ensures the PES condition given in Theorem 1. Let us define

$$b_H = a^2 + 1$$

so that the condition $\tau_0 < 0$ is equivalent to the condition $b < b_H$. Hence, Turing instability is possible if $b_T < b_H$ which is equivalent to the condition

$$\sqrt{d} < \frac{\sqrt{1 + a^2} - 1}{a}.$$

In this case, solving $\beta_k = 0$ which is equivalent to $\Delta_k = 0$ gives neutral stability curves

$$b = \frac{(a^2 + k^2)(1 + dk^2)}{k^2}.$$

This is illustrated in Figure 1.

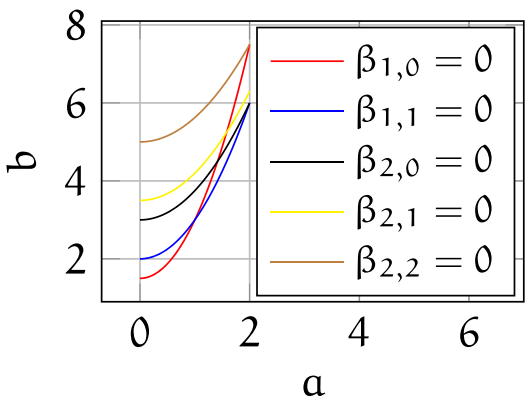

FIGURE 1 The neutral stability curves above which the eigenvalue with given wavenumber $k \in \mathcal{K}$ is unstable in the $a - b$ plane. Here, $d = 0.5$, $L = 1$ [Colour figure can be viewed at wileyonlinelibrary.com]

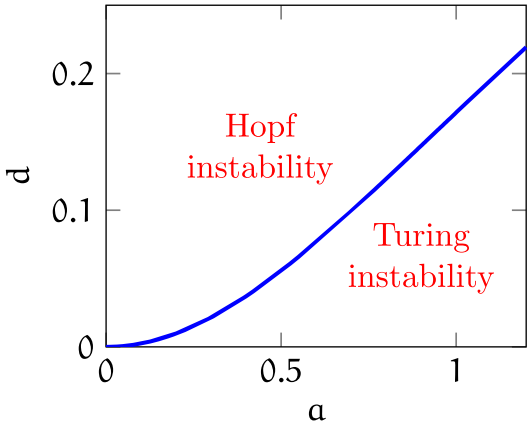

FIGURE 2 Hopf versus Turing instability in the parameter space [Colour figure can be viewed at wileyonlinelibrary.com]

As a result of the above discussion, we can write the following theorem which is known as the PES.

Theorem 1. *Suppose that* $\sqrt{d} < \frac{\sqrt{1+a^2}-1}{a}$. *Then the basic steady state is stable without diffusion, that is when* $d = 0$. *In the presence of diffusion,* $d \neq 0$, *the basic steady state loses its stability as b exceeds* $b_T = \left(a\sqrt{d}+1\right)^2$. *In particular, the linear operator has finitely many real eigenvalues with wavenumber* k_T *as defined in (28) which cross the imaginary axis as b exceeds* b_T *while the rest of its spectrum lies in the negative complex half plane.*

Another possibility of transition is the Hopf transition which occurs when $\mathrm{tr}(A) = 0$ while $\det(A) > 0$. In this case, a pair of complex eigenvalues cross the imaginary axis. It can be shown that Hopf bifurcation is possible when $\sqrt{d} > \frac{\sqrt{1+a^2}-1}{a}$; see Figure 2. However, we will not discuss this case in this study.

4 | MAIN TRANSITION THEOREMS

As illustrated in Figure 1, depending on the parameters of the system, the first critical mode(s) can have either a roll pattern or a rectangular pattern. We recall that the first critical modes have roll pattern if its wavenumber is $(k, 0)$, $k \neq 0$, or have rectangular pattern if its wavenumber is (j, k), $j \neq 0$, $k \neq 0$. Also depending on the parameters, several of these modes may become unstable simultaneously. In this paper, our aim is to identify the transitions associated with these critical crossings.

4.1 | Single rectangular mode transition

The first case we consider is a single critical mode with a rectangular spatial pattern with wavenumber $k_T = (j_1, j_2)$, $j_1 \neq 0$, $j_2 \neq 0$. Then near the onset of transition, we find that Landau equation for the amplitude of this critical mode is as follows.

$$\frac{dx}{dt} = \beta_{j_1,j_2} x_1 + A x_1^3 + o(3) \tag{30}$$

$$A = \frac{c}{16}\left(4M_{00} + 2M_{20} + 2M_{02} + M_{22}\right),\ c > 0, \tag{31}$$

and x is the time dependent amplitude of the first critical mode, and β_{j_1,j_2} is the critical eigenvalue. Moreover, the other terms are defined as follows.

$$c = \frac{(a^2 + k_T^2 + b_T)(a^2 + k_T^2)}{((a^2 + k_T^2)^2 + b_T^2)} \tag{32}$$

and the other parameter as also given by the following:

$$\begin{aligned} M_k &= \frac{(\phi_1\phi_2 + \phi_1\phi_3 v_k)V_k}{\beta_k}, \\ V_k &= \frac{v_k - 1}{v_k^2 + 1},\ v_k = \frac{-b_T}{\beta_k + a^2 + k^2}, \qquad k \in \mathcal{K}. \end{aligned} \tag{33}$$

$$\begin{aligned} \phi_1 &= \frac{(k_T^2 - a^2)b_T}{a(a^2 + k_T^2)}, \\ \phi_2 &= \frac{2k_T^2 b_T}{a(a^2 + k_T^2)}, \\ \phi_3 &= 2a. \end{aligned} \tag{34}$$

Theorem 2. *Suppose that the conditions of Theorem 1 hold and the first critical mode has a rectangular pattern with wavenumber $k_T = (j_1, j_2)$, $j_1 \neq 0$ and $j_2 \neq 0$. Then the system (2) has a transition at $b = b_T$ which depends on the number A defined in (30) and a special case of which is as shown in Figure 3. The following conclusions also hold true:*

1. *If $A > 0$ system (2) has a jump transition accompanied by subcritical pitchfork bifurcation at $b = b_T$. In particular, there are no bifurcated steady states on $b > b_T$, and there are exactly two bifurcated solutions v_+^b and v_-^b which are saddles when $b < b_T$. Also, for $b < b_T$, the stable manifolds of these bifurcated steady states divide the phase plane H into three disjoint open sets U_+^b, U_0^b, and U_-^b such that $v = 0 \in U_0^b$ is an attractor, and the orbits in $U_\pm^b$ are far from $v = 0$.*
2. *If $A < 0$ system (2) has a continuous transition accompanied by supercritical pitchfork bifurcation at $b = b_T$. In particular, there are no bifurcated steady states on $b < b_T$, and there are exactly two bifurcated solutions u_+^b and u_-^b which are attractors when $b > b_T$. Also there is a neighborhood $O \subseteq H$ of $u = 0$, such that the stable manifold of $u = 0$ divides O into two disjoint open sets U_+^b and U_-^b such that $u_+^b \in U_+^b$, $u_-^b \in U_-^b$, and $u_\pm$ attracts $U_\pm^b$.*
3. *The bifurcated steady state solutions are defined only for $\beta_{j_1,j_2}A < 0$ and are given by*

$$v_\pm^b = \pm\sqrt{\frac{-\beta_{j_1,j_2}}{A}}\cos\left(\frac{j_1 x}{L}\right)\cos j_2 y + o\left(\sqrt{-\beta_{j_1,j_2}}\right) \quad \textbf{or} \tag{35}$$

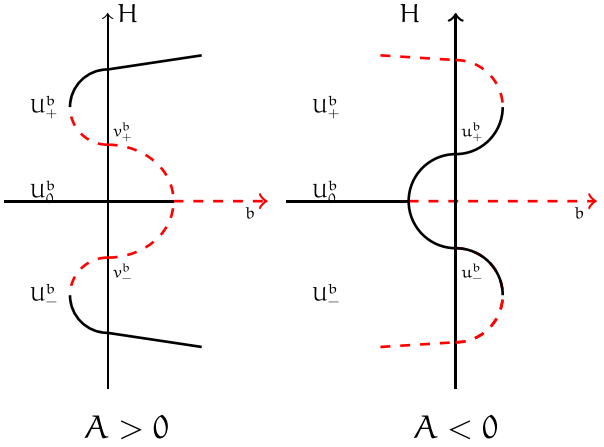

FIGURE 3 The bifurcation diagram for the Turing instability when the first critical wavenumber is $k_T = (1, 1)$. The bifurcation is subcritical pitchfork when $A > 0$ and supercritical pitchfork when $A < 0$ where A is given by (30) [Colour figure can be viewed at wileyonlinelibrary.com]

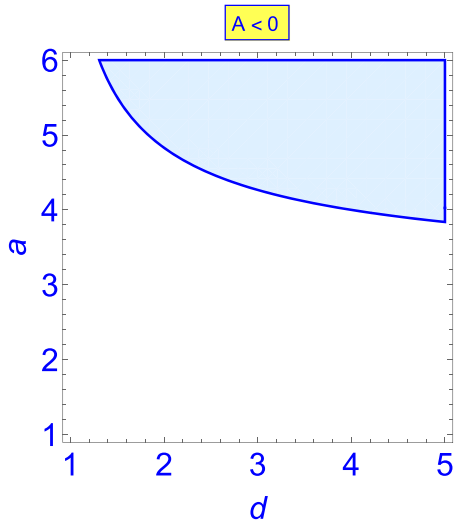

FIGURE 4 The transition type for single rectangular mode transition in the $a-d$ parameter space for the special case $j_1 = j_2 = 1$ and aspect ratio $L = 1$. The unshaded region represents **jump transition** while the shaded region represents **continuous transition** [Colour figure can be viewed at wileyonlinelibrary.com]

$$u^b_{\pm} = \pm\sqrt{\frac{-\beta_{j_1,j_2}}{A}}\cos\left(\frac{j_1 x}{L}\right)\cos j_2 y + o\left(\sqrt{-\beta_{j_1,j_2}}\right). \tag{36}$$

Figure 3 in essence summarizes Theorem 2 and displays the types of bifurcation that occurs depending on the sign of A.

To better understand the dependence of the transition number A in (31) on the system parameters, we consider a specific case where the domain is a square, the aspect ratio $L = 1$, and the first critical mode has patterns with $j_1 = j_2 = 1$. In this specific case, there exist pairs $(a, d) \in \Omega_1$ on the $a-d$ plane where $A > 0$ and pairs $(a, d) \in \Omega_2$ where $A < 0$; see Figure 4.

4.2 | Single roll mode transition

Next, we turn to the transition scenario of a single critical roll pattern mode with wavenumber

$$k_T = (j_1, 0),\ \ j_1 \neq 0.$$

In this case, our analysis shows that the Ginzburg Landau equation for this single mode is given by

$$\frac{dx_1}{dt} = \beta_{j_1,0}x_1 + Bx_1^3 + O(4) \tag{37}$$

where x_1 is the time dependent amplitude of the first critical mode and $\beta_{j_1,0}$ is the critical eigenvalue. The coefficient of the cubic term is as follows.

$$B = \frac{c}{4}(2M_{00} + M_{20}) \tag{38}$$

The transition theorem in this case is similar to that of Theorem 2, and the bifurcation diagram for the transition number B is similar to that of A. The system (2) exhibits **continuous transition** when $B < 0$ and **jump transition** when $B > 0$, see Figure 5.

The bifurcated steady state solutions defined only when $\beta_{j_1,0}B < 0$ can be expressed as

$$w^b_{\pm} = \pm\sqrt{\frac{-\beta_{j_1,0}}{B}}\cos\left(\frac{j_1 x}{L}\right) + o\left(\sqrt{-\beta_{j_1,0}}\right) \tag{39}$$

4.3 | Double roll mode transition

We consider the critical crossing of two roll modes with common wavenumber

$$k_T^2 = k_{j_1,0}^2 = k_{0,j_2}^2$$

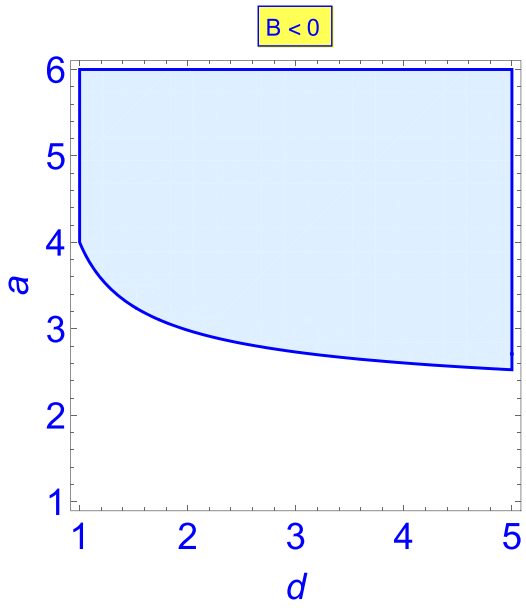

FIGURE 5 The transition type for single roll mode in the parameter space $a - d$ for the special case $j_1 = 1$ and aspect ratio $L = 1$. The unshaded region represents **jump transition** while the shaded region represents **continuous transition** [Colour figure can be viewed at wileyonlinelibrary.com]

and the critical length scale

$$L = \frac{j_1}{j_2}.$$

Then near the onset of transition, we find the Landau equations for the amplitudes of these modes as

$$\begin{aligned} \frac{dx_1}{dt} &= \beta_{j_1,0} x_1 + D_1 x_1 x_2^2 + D_2 x_1^3 + o(3) \\ \frac{dx_2}{dt} &= \beta_{0,j_2} x_2 + D_1 x_1^2 x_2 + D_3 x_2^3 + o(3) \end{aligned} \tag{40}$$

where x_1 and x_2 are the time dependent amplitudes of the critical modes and $\beta_{j_1,0}$, β_{0,j_2} are the critical eigenvalues.

$$\begin{aligned} D_1 &= \frac{c}{2}(M_{00} + 2M_{11}) \\ D_2 &= \frac{c}{4}(2M_{00} + M_{20}) \\ D_3 &= \frac{c}{4}(2M_{00} + M_{02}) \end{aligned} \tag{41}$$

Thus,

$$D_2 = B.$$

and in the case $j_1 = j_2, D_2 = D_3$. Figure 6 shows plots of D_1, D_2 in the $a - d$ parameter space.

To describe the bifurcated solutions, as in Sengul et al,[18] first we assume the following non-degeneracy conditions.

$$D_2 \neq 0,\ D_1 + D_2 \neq 0,\ \beta_{j_1,0} D_2 < 0,\ \beta_{j_1,0}(D_1 + D_2) < 0. \tag{42}$$

$$\begin{aligned} \varphi_i &= (-1)^i \sqrt{\frac{\beta_{j_1,0}}{-D_2}} \cos\left(\frac{j_1 x}{L}\right) \begin{pmatrix} 1 \\ v_{j_1,0} \end{pmatrix}, && i = 1,2 \\ \varphi_i &= (-1)^i \sqrt{\frac{\beta_{0,j_2}}{-D_2}} \cos j_2 y \begin{pmatrix} 1 \\ v_{0,j_2} \end{pmatrix}, && i = 3,4 \\ \varphi_i &= c_i \cos\left(\frac{j_1 x}{L}\right) \begin{pmatrix} 1 \\ v_{j_1,0} \end{pmatrix} + d_i \cos j_2 y \begin{pmatrix} 1 \\ v_{0,j_2} \end{pmatrix}, && i = 5,6,7,8 \end{aligned}$$

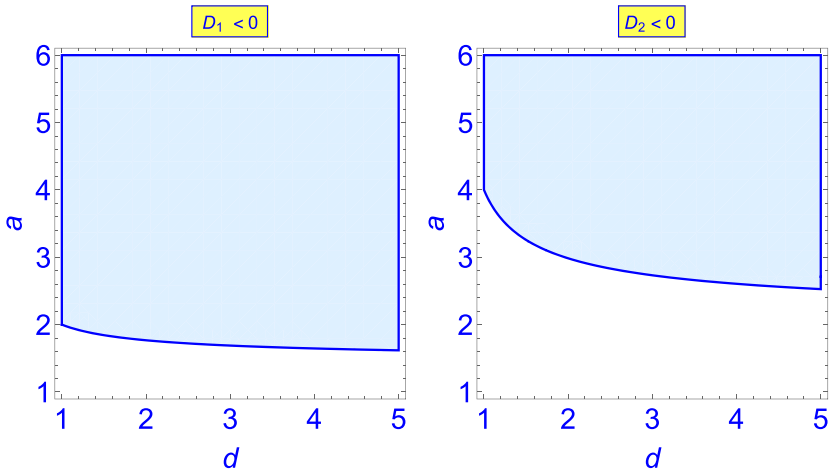

FIGURE 6 Plots of D_1(left) and D_2(right) in the $a - d$ parameter space for the case $j_1 = j_2 = 1$ and hence $D_2 = D_3$. The shaded regions, respectively, show where D_1 and D_2 are negative [Colour figure can be viewed at wileyonlinelibrary.com]

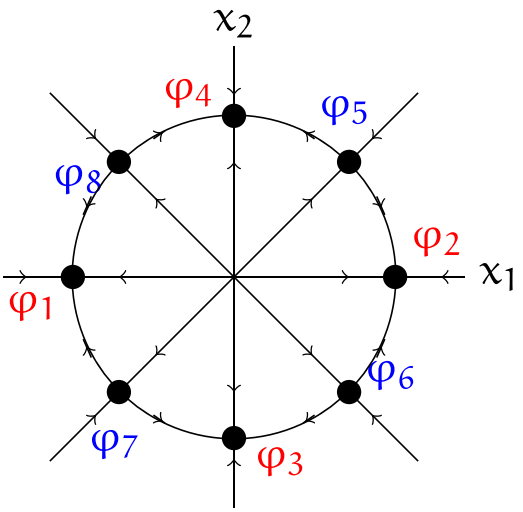

FIGURE 7 $D_1 < D_2 < 0$ [Colour figure can be viewed at wileyonlinelibrary.com]

where

$$c_5 = c_6 = -c_7 = -c_8 = \sqrt{\frac{\beta_{j_1,0}}{-(D_1 + D_2)}}$$

$$d_5 = -d_6 = d_7 = -d_8 = \sqrt{\frac{\beta_{j_1,0}}{-(D_1 + D_2)}}$$

Thus, $\varphi_1, \varphi_2, \varphi_3$, and φ_4 are the roll modes with critical wavenumber $k_T^2 = 1$ while $\varphi_5, \ldots, \varphi_8$ are mixed modes which are the superposition of the roll modes.

Theorem 3. *Assume the aspect ratio is $L = j_1/j_2$ and the first two critical modes have wavenumbers $k_T = (j_1, 0)$ and $k_T = (0, j_2)$ such that $j_1 = j_2$. Then the system undergoes a first transition as b exceeds b_T. Moreover, under the assumption (42), the system has a continuous (respectively jump) transition accompanied by a bifurcated attractor (respectively repeller) Σ_b on $b > b_T$ (respectively, on $b < b_T$) depending on D_1, D_2. Σ_b is homeomorphic to the circle S^1 and contains the steady states together with connecting heteroclinic orbits.*

We let $N(\Sigma_b)$ denote the number of steady states on Σ_b, S denotes stable steady states, and U denotes the unstable steady states on Σ_b. We have the following characterization of Σ_b which is also given in Figures 7 and 8.

(i) If $D_1 < D_2 < 0$, then Σ_b is an attractor such that $N(\Sigma_b) = 8$, $S = \{\varphi_i | i = 1, 2, 3, 4\}$, $U = \{\varphi_i | i = 5, 6, 7, 8\}$.
(ii) If $D_2 < D_1 < 0$ or $D_2 < 0 < D_1$ $D_1 + D_2 < 0$, then Σ_b is an attractor such that $N(\Sigma_b) = 8$, $S = \{\varphi_i | i = 5, 6, 7, 8\}$, $U = \{\varphi_i | i = 1, 2, 3, 4\}$.
(iii) If $D_2 < 0 < D_1$, $D_1 + D_2 > 0$, then Σ_b is a repeller such that $N(\Sigma_b) = 4$, $U = \{\varphi_i | i = 1, 2, 3, 4\}$.

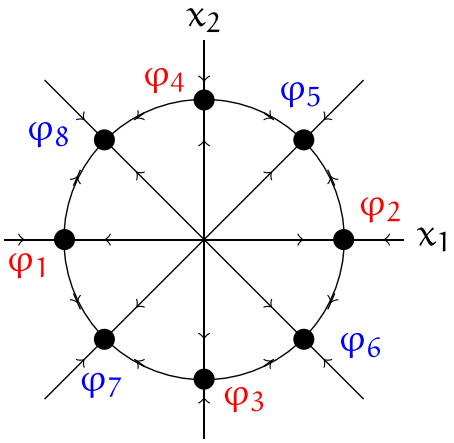

FIGURE 8 $D_2 < D_1 < 0$ (or $D_2 < 0 < D_1$), $D_1 + D_2 < 0$ [Colour figure can be viewed at wileyonlinelibrary.com]

Steady state	Existence condition	Stability condition
φ_1, φ_2	$\beta_{j_1,0} D_2 < 0$	$D_1 < D_2 < 0$
φ_3, φ_4	$\beta_{0,j_2} D_2 < 0$	$D_1 < D_2 < 0$
$\varphi_5, \varphi_6, \varphi_7, \varphi_8$	$\beta_{j_1,0}(D_1 + D_2) < 0$, $\beta_{0,j_2}(D_1 + D_2) < 0$	$D_2 < D_1 < 0$

TABLE 1 Existence and stability conditions for steady states of the double roll mode transitions

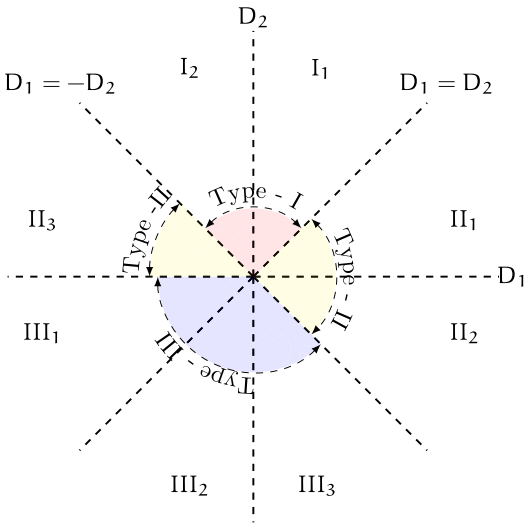

FIGURE 9 Classification of transition types for the double roll mode: Continuous Type-I, Jump Type-II, Mixed Type III. See Figures 7 and 8 for the topological structures of III_1, III_2, and III_3 [Colour figure can be viewed at wileyonlinelibrary.com]

(iv) *If $D_2 > D_1 > 0$, then Σ_b is a repeller such that $N(\Sigma_b) = 4$, $U = \{\varphi_i | i = 5, 6, 7, 8\}$.*
(v) *If $D_2 > 0 > D_1$, $D_1 + D_2 < 0$, then Σ_b is a repeller such that $N(\Sigma_b) = 4$, $U = \{\varphi_i | i = 5, 6, 7, 8\}$.*
(vi) *$D_2 > 0 > D_1$ or $D_2 > D_1 > 0$, $D_1 + D_2 > 0$, then Σ_b is an attractor such that $N(\Sigma_b) = 4$, $S = \{\varphi_i | i = 5, 6, 7, 8\}$.*

From Theorem 3, the structure of the attractor depends on the signs of D_1, D_2. Figures 7 and 8 show the possible transitions from Theorem 3. Table 1 provides the summary of the steady states, condition of existence, and stability (Figure 9).

4.4 | A roll and a rectangular mode transition

Now we consider the interactions of a roll mode with a square mode. To understand the formation of hexagonal patterns, we let the critical wavenumber be as follows.

$$k_T^2 = k_{2j_1,0}^2 = k_{j_1,j_2}^2 \tag{43}$$

Such that the critical length scale,

$$L = \frac{j_1 \sqrt{3}}{j_2}.$$

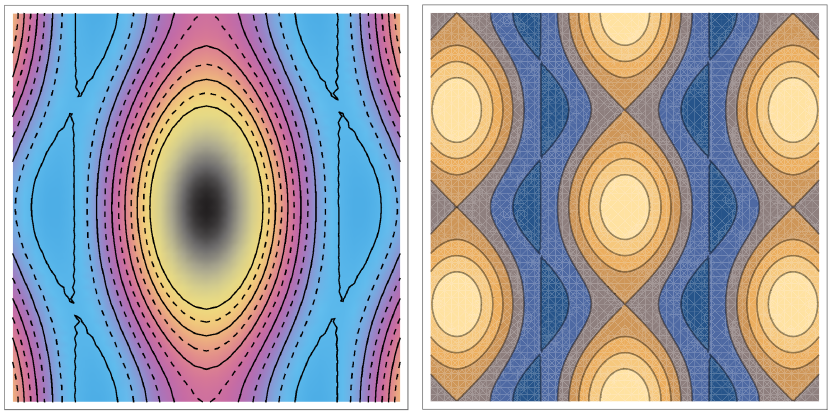

FIGURE 10 Density plot (left), contour plot (right) of sample mixed mode patterns, $\cos\left(x/\sqrt{3}\right)\cos(y)+\cos\left(2x/\sqrt{3}\right)$ as applied to Theorem 4 [Colour figure can be viewed at wileyonlinelibrary.com]

Moreover, we assume that one of the first two critical modes has a square pattern, and the other has a roll pattern.

Under the above assumptions and near $b=b_T$, we let $\beta_{j_1,0}=\beta_{j_1,j_2}=\beta$, then we obtain that the dynamics of the system is dictated by the following ODE system

$$\begin{aligned}\frac{dx_1}{dt}&=\beta x_1+A_1x_1x_2+x_1(A_2x_1^2+A_3x_2^2)+O(4)\\ \frac{dx_2}{dt}&=\beta x_2+B_1x_1^2+x_2(B_2x_1^2+B_3x_2^2)+O(4)\end{aligned}\tag{44}$$

$$\begin{aligned}A_1&=c\phi_1,\quad A_2=\frac{c}{16}\left(M_{22}+4M_{00}\right),\quad A_3=\frac{c}{2}\left(M_{00}+2M_{31}\right)\\ B_1&=\frac{c\phi_1}{4},\quad B_2=\frac{c}{2}\left(M_{00}+2M_{31}\right),\quad B_3=\frac{c}{4}\left(2M_{00}+M_{40}\right)\end{aligned}\tag{45}$$

Thus from (45), we observe that $A_1=4B_1$ and $A_3=B_2$.

For the analysis of (44), we assume the following non-degeneracy conditions.

$$B_3\neq 0,\qquad A_1B_1\neq 0.\tag{46}$$

To discuss the bifurcated steady states, we define the following pure and mixed solutions.

$$\begin{aligned}\varphi_i&=(-1)^i\sqrt{-\frac{\beta}{B_3}}\cos(j_2y)\begin{pmatrix}1\\ v_{0,j_2}\end{pmatrix},\qquad i=1,2\\ \varphi_i&=(-1)^i\frac{1}{\sqrt{A_1B_1}}\beta\cos\left(\frac{j_1x}{L}\right)\cos(j_2y)\begin{pmatrix}1\\ v_{j_1,j_2}\end{pmatrix}-\frac{1}{A_1}\beta\cos(j_2y)\begin{pmatrix}1\\ v_{0,j_2}\end{pmatrix},\ i=3,4\end{aligned}$$

Thus φ_1,φ_2 are the pure modes modes while φ_3,φ_4 are the mixed modes. In what follows, we provide the key aspects of the transition theory of system (44). We note that the transition of the system depends on the coefficients A_1,B_2, and B_3 while the rest of the coefficients only play quantitative role. For full details of the theorem, the stability and existence of the steady states as well as the related transition diagrams and detailed analysis, we refer the interested reader to Şengül[16] and the proofs there in (Figure 10).

Theorem 4. ***For*** $A_1B_1>0$,

(i) If $B_3<0$, then the system (44) undergoes a random (Type-III) transition near $b=b_T$.
(ii) If $B_3>0$, then the system (44) undergoes a catastrophic (Type-II) transition at $b=b_T$.

For $A_1B_1<0$,

(i) If $B_3<0$, then the system (44) undergoes a continuous (Type-I) transition near $b=b_T$.
(ii) If $B_3>0$, then the system (44) undergoes a catastrophic (Type-II) transition at $b=b_T$.

5 | PROOFS

In this section, we present the proofs of our main theorems using the center manifold reduction criteria to establish amplitude equations for various modes of transitions.

5.1 | Center manifold reduction

We write our solution as follows.

$$\begin{pmatrix} u \\ v \end{pmatrix} = \sum_{k=1}^{r} x_k \begin{pmatrix} u_k \\ v_k \end{pmatrix} e_{k_1,k_2} + \begin{pmatrix} \Phi_u \\ \Phi_v \end{pmatrix} \tag{47}$$

where r is the number of critical modes while Φ_u and Φ_v are the u and v components of the center manifold function.

$$e_{k_1,k_2} = \cos\frac{k_1}{L}x\cos k_2 y$$

We adopt the following notations for simplicity.

$$e_{mn} = \cos\left(\frac{mj_1x}{L}\right)\cos(nj_2y)\ m,n \in \mathbb{Z}^+ \cup \{0\}$$
$$f_{mn} = e_{mn}$$

For example, $f_{20} = e_{2j_10}$, $f_{11} = e_{j_1j_2}$.

5.1.1 | Single rectangular mode transition

We consider a single critical mode with rectangular pattern

$$f_{11} = e_{j_1j_2} = \cos\frac{j_1}{L}x\cos j_2 y$$

$$\begin{pmatrix} u \\ v \end{pmatrix} = x(t)\begin{pmatrix} u_{j_1,j_2} \\ v_{j_1,j_2} \end{pmatrix} f_{11} + \begin{pmatrix} \Phi_u \\ \Phi_v \end{pmatrix} \tag{48}$$

where $\begin{pmatrix} u_{j_1,j_2} \\ v_{j_1,j_2} \end{pmatrix} f_{11}$ is the critical eigenvector and

$$\begin{aligned} \begin{pmatrix} \Phi_u \\ \Phi_v \end{pmatrix} = \Phi_{00}\begin{pmatrix} u_{0,0} \\ v_{0,0} \end{pmatrix} f_{00} + \Phi_{20}\begin{pmatrix} u_{2j_1,0} \\ v_{2j_1,0} \end{pmatrix} f_{20} \\ + \Phi_{02}\begin{pmatrix} u_{0,2j_2} \\ v_{0,2j_2} \end{pmatrix} f_{02} + \Phi_{22}\begin{pmatrix} u_{2j_1,2j_2} \\ v_{2j_1,2j_2} \end{pmatrix} f_{22} \end{aligned} \tag{49}$$

where

$$\begin{aligned} \Phi_{00} &= q_{00}x^2 \\ \Phi_{20} &= q_{20}x^2 \\ \Phi_{02} &= q_{02}x^2 \\ \Phi_{22} &= q_{22}x^2. \end{aligned} \tag{50}$$

By substituting the central part of (48) into (11), we have

$$f_{11}\begin{pmatrix} u_{j_1,j_2} \\ v_{j_1,j_2} \end{pmatrix}\frac{dx(t)}{dt} = x\begin{pmatrix} u_{j_1,j_2} \\ v_{j_1,j_2} \end{pmatrix}\beta_{j_1,j_2}f_{11} + \begin{pmatrix} g_1(u,v) \\ g_2(u,v) \end{pmatrix} \tag{51}$$

where

$$G(\mathbf{u}) = \begin{pmatrix} g_1(u,v) \\ g_2(u,v) \end{pmatrix}.$$

We take the inner product of (51) with $\begin{pmatrix} u_{j_1,j_2} \\ v_{j_1,j_2} \end{pmatrix} f_{11}$ and obtain the following equation.

$$\begin{aligned} \frac{dx(t)}{dt} &= \beta_{j_1,j_2} x(t) + \left(\frac{1 - v_{j_1,j_2}}{1 + v_{j_1,j_2}^2} \right) \frac{\langle g_1(u,v), f_{11} \rangle}{\langle f_{11}, f_{11} \rangle} \\ \frac{dx(t)}{dt} &= \beta_{j_1,j_2} x(t) + c \frac{\langle g_1(u,v), f_{11} \rangle}{\langle f_{11}, f_{11} \rangle} \end{aligned} \tag{52}$$

where c is a positive constant given by

$$c = \left(\frac{1 - v_{j_1,j_2}}{1 + v_{j_1,j_2}^2} \right) = \frac{(a^2 + k_T^2 + b_T)(a^2 + k_T^2)}{((a^2 + k_T^2)^2 + b_T^2)}$$

$$\begin{aligned} g_1(u,v) &= \frac{b}{a} u^2 + 2auv + h.o.t \\ &= \left(\frac{b}{a} + 2av_{j_1,j_2} \right) x_1^2 f_{11}^2 + \left(2\frac{b}{a} + 2av_{j_1,j_2} \right) x_1 f_{11} \Phi_u + 2ax_1 f_{11} \Phi_v \\ &= \phi_1 x_1^2 f_{11}^2 + \phi_2 x_1 f_{11} \Phi_u + \phi_3 x_1 f_{11} \Phi_v \end{aligned} \tag{53}$$

$\phi_i, i = 1, 2, 3$ are as defined in (34), and we have made the substitution $u_{11} = 1$.
We define G_{21} as the quadratic part of $g_1(u,v)$ as follows.

$$G_{21} = \phi_1 x_1^2 f_{11}^2 \tag{54}$$

Also

$$\langle f_1, f_2, f_3 \rangle = \int_\Omega (f_1 f_2 f_3) d\mu, \ \langle f_1, f_2 \rangle = \int_\Omega (f_1 f_2) d\mu$$

$$\langle g_1, f_{11} \rangle = \phi_1 x_1^2 \langle f_{11}^2, f_{11} \rangle + \phi_2 x_1 \langle f_{11} \Phi_u, f_{11} \rangle + \phi_3 x_1 \langle f_{11} \Phi_v, f_{11} \rangle \tag{55}$$

The inner products in (55) are as follows.

$$\begin{aligned} \langle f_{11} \Phi_u, f_{11} \rangle &= \Phi_{00} \langle f_{11} f_{00}, f_{11} \rangle + \Phi_{20} \langle f_{11} f_{20}, f_{11} \rangle + \Phi_{02} \langle f_{11} f_{02}, f_{11} \rangle \\ &\quad + \Phi_{22} \langle f_{11} f_{22}, f_{11} \rangle \\ &= \frac{L\pi^2}{16} \left(4\Phi_{0,0} + 2\Phi_{20} + 2\Phi_{02} + \Phi_{22} \right) \\ \langle f_{11} \Phi_v, f_{11} \rangle &= \Phi_{00} v_{0,0} \langle f_{11} f_{00}, f_{11} \rangle \Phi_{20} v_{2j_1,0} \langle f_{11} f_{20}, f_{11} \rangle + \Phi_{02} v_{0,2j_2} \langle f_{11} f_{02}, f_{11} \rangle \\ &\quad + \Phi_{22} v_{2j_1,2j_2} \langle f_{11} f_{22}, f_{11} \rangle \\ &= \frac{L\pi^2}{16} \left(4\Phi_{0,0} v_{0,0} + 2\Phi_{20} v_{2j_1,0} + 2\Phi_{02} v_{0,2j_2} + \Phi_{22} v_{2j_1,2j_2} \right) \\ \langle f_{11}^2, f_{11} \rangle &= 0. \end{aligned} \tag{56}$$

Next we substitute (56) into (55) and obtain the following.

$$\langle g_1, f_{11}\rangle = \frac{L\pi^2}{16}\left[4(\phi_2+\phi_3 v_{0,0})\Phi_{00} + 2(\phi_2+\phi_3 v_{2j_1,0})\Phi_{20} + 2(\phi_2+\phi_3 v_{0,2j_2})\Phi_{02} + (\phi_2+\phi_3 v_{2j_1,2j_2})\Phi_{22}\right]x_1 \tag{57}$$

Next we solve for the coefficients of the center manifold functions by first evaluating the following inner products.

$$\begin{aligned}
&\langle G_{21}, f_{00}\rangle = 4\langle G_{21}, f_{22}\rangle = \frac{L\pi^2}{4}\phi_1 x_1^2\\
&\langle G_{21}, f_{20}\rangle = \langle G_{21}, f_{02}\rangle = \frac{L\pi^2}{8}\phi_1 x_1^2\\
&\langle f_{11}, f_{11}\rangle = \langle f_{22}, f_{22}\rangle = \frac{L\pi^2}{4}\\
&\langle f_{20}, f_{20}\rangle = \langle f_{02}, f_{02}\rangle = \frac{L\pi^2}{2}\\
&\langle f_{11}^2, f_{11}\rangle = 0
\end{aligned} \tag{58}$$

then utilizing the equation

$$\frac{d\Phi}{dt} = L(\Phi) + G(u)$$

that is,

$$\frac{d}{dt}\begin{bmatrix}\Phi_u\\ \Phi_v\end{bmatrix} = L\begin{bmatrix}\Phi_u\\ \Phi_v\end{bmatrix} + \begin{bmatrix}G_{21}\\ G_{22}\end{bmatrix} \tag{59}$$

Substituting the terms of the center manifold function in turns, we have

$$\begin{aligned}
f_{20}\begin{pmatrix}u_{2j_1,0}\\ v_{2j_1,0}\end{pmatrix}\frac{d\Phi_{20}}{dt} &= \beta_{2j_1,0}\Phi_{20}\begin{pmatrix}u_{2j_1,0}\\ v_{2j_1,0}\end{pmatrix} f_{20} + P_2\begin{pmatrix}G_{21}\\ G_{22}\end{pmatrix}\\
\frac{d\Phi_{20}}{dt} &= \beta_{2j_1,0}\Phi_{20} + \left(\tfrac{1-v_{2j_1,0}}{1+v_{2j_1,0}^2}\right)\frac{\langle G_{21}, f_{20}\rangle}{\langle f_{20}, f_{20}\rangle}\\
&= \beta_{2j_1,0}q_{20}x_1^2 + \left(\tfrac{1-v_{2j_1,0}}{1+v_{2j_1,0}^2}\right)\frac{\langle G_{21}, f_{20}\rangle}{\langle f_{20}, f_{20}\rangle}
\end{aligned} \tag{60}$$

$$\begin{aligned}
\frac{d\Phi_{20}}{dt} &= \frac{\partial\Phi_{20}}{dt}.\frac{dx_1}{dt}\\
&= 2q_{20}x_1(\beta_{j_1,j_2}x_1 + \dots)
\end{aligned} \tag{61}$$

By comparing (60) and (61) and following similar computations, we can write the coefficients as follows.

$$\begin{aligned}
q_{00} &= \frac{\phi_1}{4\beta_{0,0}}V_{0,0}, & \Phi_{00} &= \frac{\phi_1}{4\beta_{0,0}}V_{0,0}x_1^2\\
q_{20} &= \frac{\phi_1}{4\beta_{2j_1,0}}V_{2j_1,0}, & \Phi_{20} &= \frac{\phi_1}{4\beta_{2j_1,0}}V_{2j_1,0}x_1^2,\\
q_{02} &= \frac{\phi_1}{4\beta_{0,2j_2}}V_{0,2j_2}, & \Phi_{02} &= \frac{\phi_1}{4\beta_{0,2j_2}}V_{0,2j_2}x_1^2,\\
q_{22} &= \frac{\phi_1}{4\beta_{2j_1,2j_2}}V_{2j_1,2j_2}, & \Phi_{22} &= \frac{\phi_1}{4\beta_{2j_1,2j_2}}V_{2j_1,2j_2}x_1^2
\end{aligned} \tag{62}$$

Thus, (57) can be simplified to

$$\langle g_1, f_{11}\rangle = \frac{L\pi^2}{64}(4M_{00} + 2M_{20} + 2M_{02} + M_{22})x_1^3 \tag{63}$$

where M_{00}, M_{20}, M_{02}, and M_{22} are as defined in (33). When we substitute (63) into (52), we obtain (30). This concludes the proof for this case.

5.1.2 | Single roll mode transition

We consider a single critical mode with roll pattern.

$$f_{10} = e_{j_1,0} = \cos\left(\frac{j_1 x}{L}\right),\ j_1 \in \mathbb{N}$$

$$\begin{pmatrix} u \\ v \end{pmatrix} = x_1 \begin{pmatrix} u_{j_1,0} \\ v_{j_1,0} \end{pmatrix} f_{10} + \begin{pmatrix} \Phi_u \\ \Phi_v \end{pmatrix} \tag{64}$$

$$\begin{aligned} \begin{pmatrix} \Phi_u \\ \Phi_v \end{pmatrix} = \Phi_{00} \begin{pmatrix} u_{0,0} \\ v_{0,0} \end{pmatrix} f_{00} + \Phi_{20} \begin{pmatrix} u_{2j_1,0} \\ v_{2j_1,0} \end{pmatrix} f_{20} \\ + \Phi_{02} \begin{pmatrix} u_{0,2j_2} \\ v_{0,2j_2} \end{pmatrix} f_{02} + \Phi_{11} \begin{pmatrix} u_{j_1,j_2} \\ v_{j_1,j_2} \end{pmatrix} f_{11} \end{aligned} \tag{65}$$

$$\begin{aligned} \Phi_{00} &= m_{00} x_1^2 \\ \Phi_{20} &= m_{20} x_1^2 \\ \Phi_{02} &= m_{02} x_1^2 \\ \Phi_{11} &= m_{22} x_1^2 \end{aligned}$$

By substituting the center part of the solution (64) into (11), we obtain the following amplitude equations.

$$\frac{dx_1}{dt} = \beta_{j_1,0} x_1 + c \frac{\langle g_1, f_{10} \rangle}{\langle f_{10}, f_{10} \rangle} \tag{66}$$

Following similar process as in the single rectangular mode transition, we can show that in this case,

$$\begin{aligned} g_1 &= \phi_1 x_1^2 f_{10}^2 + \phi_2 x_1 f_{10} \Phi_u + \phi_3 x_1 f_{10} \Phi_v \\ \langle g_1, f_{10} \rangle &= \phi_1 x_1^2 \langle f_{10}^2, f_{10} \rangle + \phi_2 x_1 \langle f_{10} \Phi_u, f_{10} \rangle + \phi_3 x_1 \langle f_{10} \Phi_v, f_{10} \rangle \\ \langle g_1, f_{10} \rangle &= \frac{L\pi^2}{4} \left[(\phi_2 + \phi_3 v_{2j_1,0}) \Phi_{20} + (\phi_2 + \phi_3 v_{0,0}) \Phi_{00} \right] x_1 \\ &= \frac{L\pi^2}{4} \left(M_{00} + 1/2 M_{20} \right) x_1^3, \\ \langle f_{10}, f_{10} \rangle &= \frac{L\pi^2}{2},\ \langle f_{10}^2, f_{10} \rangle = 0,\ \langle f_{00}, f_{00} \rangle = L\pi^2. \end{aligned} \tag{67}$$

The coefficients of the center manifold function are computed in a similar fashion as in the single rectangular mode transition.

$$\begin{aligned} m_{00} &= \frac{\phi_1}{2\beta_{00}} V_{00}, & \Phi_{00} &= \frac{\phi_1}{2\beta_{00}} V_{00} x_1^2, \\ m_{20} &= \frac{\phi_1}{4\beta_{2j_1,0}} V_{2j_1,0}, & \Phi_{20} &= \frac{\phi_1}{4\beta_{2j_1,0}} V_{2j_1,0} x_1^2, \\ m_{02} &= m_{22} = 0. \end{aligned} \tag{68}$$

Substituting the results in (67) into (66), we obtain the results in (38). This concludes the proof.

5.1.3 | Transitions from double roll mode

In this case, $r = 2$, and the critical modes are

$$f_{10} = e_{j_1,0} = \cos\left(\frac{j_1 x}{L}\right),\ f_{01} = e_{0,j_2} = \cos j_2 y,\ j_1, j_2 \in \mathbb{N}$$

$$\begin{pmatrix} u \\ v \end{pmatrix} = x_1(t)\begin{pmatrix} u_{j_1,0} \\ v_{j_1,0} \end{pmatrix} f_{10} + x_2(t)\begin{pmatrix} u_{0,j_2} \\ v_{0,j_2} \end{pmatrix} f_{01} + \begin{pmatrix} \Phi_u \\ \Phi_v \end{pmatrix} \tag{69}$$

$$\begin{pmatrix} \Phi_u \\ \Phi_v \end{pmatrix} = \Phi_{00}\begin{pmatrix} u_{0,0} \\ v_{0,0} \end{pmatrix} f_{00} + \Phi_{20}\begin{pmatrix} u_{2j_1,0} \\ v_{2j_1,0} \end{pmatrix} f_{20} + \Phi_{02}\begin{pmatrix} u_{0,2j_2} \\ v_{0,2j_2} \end{pmatrix} f_{02} + \Phi_{11}\begin{pmatrix} u_{j_1,j_2} \\ v_{j_1,j_2} \end{pmatrix} f_{11}$$

$$\begin{aligned} \Phi_{20}(x_1,x_2) &= a_{11}x_1^2 + a_{12}x_1x_2 + a_{22}x_2^2 \\ \Phi_{02}(x_1,x_2) &= b_{11}x_1^2 + b_{12}x_1x_2 + b_{22}x_2^2 \\ \Phi_{11}(x_1,x_2) &= c_{11}x_1^2 + c_{12}x_1x_2 + c_{22}x_2^2 \\ \Phi_{00}(x_1,x_2) &= d_{11}x_1^2 + d_{12}x_1x_2 + d_{22}x_2^2 \end{aligned}.$$

By substituting the center part of the solution into (11), we obtain the following amplitude equations.

$$\begin{aligned} \frac{dx_1}{dt} &= \beta_{j_1,0}x_1 + c\frac{\langle g_1, f_{10}\rangle}{\langle f_{10}, f_{10}\rangle} \\ \frac{dx_2}{dt} &= \beta_{0,j_2}x_2 + c\frac{\langle g_1, f_{01}\rangle}{\langle f_{01}, f_{01}\rangle} \end{aligned} \tag{70}$$

where c is as defined in (32), whereas in this case, $g_1(u,v)$ is defined as

$$g_1(u,v) = \left(x_1^2 f_{10}^2 + 2x_1x_2f_{10}f_{01} + x_2f_{01}^2\right)\phi_1 + (x_1f_{10} + x_2f_{01})(\phi_2\Phi_u + \phi_3\Phi_v). \tag{71}$$

In this case, the quadratic part of $g_1(u,v)$ is given by

$$G_{21} = \left(x_1^2 f_{10}^2 + 2x_1x_2f_{10}f_{01} + x_2^2f_{01}^2\right)\phi_1.$$

Now we evaluate $\langle g_1, f_{10}\rangle$ and $\langle g_1, f_{01}\rangle$ as follows.

$$\begin{aligned} \langle g_1, f_{10}\rangle &= \phi_1\rho_1 + \phi_2\rho_2 + \phi_3\rho_3 \\ \rho_1 &= \langle\left(x_1^2f_{10}^2 + 2x_1x_2f_{10}f_{01} + x_2^2f_{01}^2\right), f_{10}\rangle \\ \rho_2 &= \langle(x_1f_{10} + x_2f_{01})\Phi_u, f_{10}\rangle \\ \rho_3 &= \langle(x_1f_{10} + x_2f_{01})\Phi_v, f_{10}\rangle \end{aligned}. \tag{72}$$

$$\begin{aligned} \langle g_1, f_{01}\rangle &= \phi_1\tilde{\rho}_1 + \phi_2\tilde{\rho}_2 + \phi_3\tilde{\rho}_3 \\ \tilde{\rho}_1 &= \langle\left(x_1^2f_{10}^2 + 2x_1x_2f_{10}f_{01} + x_2^2f_{01}^2\right), f_{01}\rangle \\ \tilde{\rho}_2 &= \langle(x_1f_{10} + x_2f_{01})\Phi_u, f_{01}\rangle \\ \tilde{\rho}_3 &= \langle(x_1f_{10} + x_2f_{01})\Phi_v, f_{01}\rangle \end{aligned}. \tag{73}$$

Hence, (72) and (73) evaluate to

$$\begin{aligned} \langle g_1, f_{10}\rangle &= \frac{L\pi^2}{4}\left[2(\phi_2 + \phi_3v_{00})\Phi_{00}x_1 + \left(\phi_2 + \phi_3v_{2j_1,0}\right)\Phi_{20}x_1 + \left(\phi_2 + \phi_3v_{j_1,j_2}\right)\Phi_{11}x_2\right] \\ \langle g_1, f_{01}\rangle &= \frac{L\pi^2}{4}\left[2(\phi_2 + \phi_3v_{00})\Phi_{00}x_2 + \left(\phi_2 + \phi_3v_{0,2j_2}\right)\Phi_{02}x_2 + \left(\phi_2 + \phi_3v_{j_1,j_2}\right)\Phi_{11}x_1\right] \end{aligned}. \tag{74}$$

$$\langle G_{21}, f_{20}\rangle = \frac{L\pi^2}{4}\phi_1 x_1^2,\ \langle f_{20}, f_{20}\rangle = \frac{L\pi^2}{2}$$
$$\langle G_{21}, f_{02}\rangle = \frac{L\pi^2}{4}\phi_1 x_2^2,\ \langle f_{02}, f_{02}\rangle = \frac{L\pi^2}{2}$$
$$\langle G_{21}, f_{11}\rangle = \frac{L\pi^2}{2}\phi_1 x_1 x_2,\ \langle f_{11}, f_{11}\rangle = \frac{L\pi^2}{4}$$
$$\langle G_{21}, f_{00}\rangle = \frac{L\pi^2}{4}\phi_1 (x_1^2 + x_2^2),\ \langle f_{00}, f_{00}\rangle = L\pi^2$$

Now we look for the coefficients of the terms in the center manifold function. We substitute each of the terms of center manifold part of our solution to (11) and take the inner product with respect to respective eigenfunctions as in the previous cases, and we obtain the following equations.

$$\begin{aligned}
\frac{d\Phi_{20}(x_1,x_2)}{dt} &= \beta_{2j_1,0}\Phi_{20} + \left(\frac{1-v_{20}}{1+v_{20}^2}\right)\frac{\langle G_{21}, f_{20}\rangle}{\langle f_{20}, f_{20}\rangle}\\
\frac{d\Phi_{02}(x_1,x_2)}{dt} &= \beta_{0,2j_2}\Phi_{02} + \left(\frac{1-v_{02}}{1+v_{02}^2}\right)\frac{\langle G_{21}, f_{02}\rangle}{\langle f_{02}, f_{02}\rangle}\\
\frac{d\Phi_{11}(x_1,x_2)}{dt} &= \beta_{j_1,j_2}\Phi_{11} + \left(\frac{1-v_{11}}{1+v_{11}^2}\right)\frac{\langle G_{21}, f_{11}\rangle}{\langle f_{11}, f_{11}\rangle}
\end{aligned} \tag{75}$$

Equation (75) can also be written alternatively as

$$\begin{aligned}
\frac{d\Phi_{00}}{dt} &= \frac{\partial\Phi_{00}}{\partial x_1}\cdot\frac{dx_1}{dt} + \frac{\partial\Phi_{00}}{\partial x_2}\cdot\frac{dx_2}{dt}\\
\frac{d\Phi_{20}}{dt} &= \frac{\partial\Phi_{20}}{\partial x_1}\cdot\frac{dx_1}{dt} + \frac{\partial\Phi_{20}}{\partial x_2}\cdot\frac{dx_2}{dt}\\
\frac{d\Phi_{02}}{dt} &= \frac{\partial\Phi_{02}}{\partial x_1}\cdot\frac{x_1}{dt} + \frac{\partial\Phi_{02}}{\partial x_2}\cdot\frac{dx_2}{dt}\\
\frac{d\Phi_{11}}{dt} &= \frac{\partial\Phi_{11}}{\partial x_1}\cdot\frac{dx_1}{dt} + \frac{\partial\Phi_{11}}{\partial x_2}\cdot\frac{dx_2}{dt}
\end{aligned} \tag{76}$$

By comparing (75) and (76), we obtain the following results for the coefficients.

$$\begin{aligned}
d_{11} = d_{11} &= \frac{\phi_1}{2\beta_{0,0}}V_{0,0},\ d_{12} = 0\\
a_{11} &= \frac{\phi_1}{2\beta_{2j_1,0}}V_{2j_1,0},\ a_{12} = a_{22} = 0\\
b_{22} &= \frac{\phi_1}{2\beta_{0,2j_2}}V_{0,2j_2},\ b_{11} = b_{12} = 0\\
c_{12} &= \frac{2\phi_1}{\beta_{j_1,j_2}}V_{j_1,j_2},\ c_{11} = c_{22} = 0
\end{aligned} \tag{77}$$

Substituting (77) into (74), we obtain

$$\begin{aligned}
\langle g_1, f_{10}\rangle &= \frac{L\pi^2}{4}\left[(M_{00} + 1/2M_{20})x_1^3 + (M_{00} + 2M_{11})x_1x_2^2\right]\\
\langle g_1, f_{01}\rangle &= \frac{L\pi^2}{4}\left[(M_{00} + 2M_{11})x_1^2x_2 + (M_{00} + 1/2M_{02})x_2^3\right]
\end{aligned} \tag{78}$$

By putting (78) into (70) simplifies to (40).

The steady states for (40) are as follows.

$$\begin{aligned} P_0 &= (0,0) \\ P_1^{\pm} &\equiv \left(0, \pm\sqrt{\frac{-\beta_{j_1,0}}{D_2}}\right), \ \beta_{j_1,0}D_2 < 0 \\ P_2^{\pm} &\equiv \left(\pm\sqrt{\frac{-\beta_{j_1,0}}{D_2}}, 0\right), \ \beta_{10}D_2 < 0 \\ M^{\pm} &\equiv \left(\pm\sqrt{\frac{-\beta_{j_1 0}}{D_1+D_2}}, \pm\sqrt{\frac{-\beta_{j_1,0}}{D_1+D_2}}\right), \ \beta_{j_1,0}(D_1+D_2) < 0 \end{aligned} \quad . \tag{79}$$

$P_1^{\pm}$ and $P_2^{\pm}$ are steady states for the pure modes while $M^{\pm}$ represents the steady states of the mixed modes. We define the Jacobian,

$$J(x_1,x_2) = \begin{bmatrix} \beta_{j_1,0} + D_1x_2^2 + 3D_2x_1^2 & 2D_1x_1x_2 \\ 2D_1x_1x_2 & \beta_{j_1,0} + D_1x_1^2 + 3D_2x_2^2 \end{bmatrix}. \tag{80}$$

$$J(P_0) = \begin{bmatrix} \beta_{j_1,0} & 0 \\ 0 & \beta_{j_1,0} \end{bmatrix}. \tag{81}$$

P_0 is unstable if $\lambda_0 = \beta_{j_1,0} > 0$ and stable if $\lambda_0 = \beta_{j_1,0} < 0$.

$$J(P_1^{\pm}) = \begin{bmatrix} \frac{(D_2-D_1)}{D_2}\beta_{j_1,0} & 0 \\ 0 & -2\beta_{j_1,0} \end{bmatrix} \tag{82}$$

From (79), $\lambda_1^{P_1} = 1/D_2(D_2-D_1)\beta_{j_1,0}$ and $\lambda_2^{P_1} = -2\beta_{j_1,0}$ and also from (80), $\lambda_2^{P_1} = -2\beta_{j_1,0}$ and $\lambda_1^{P_2} = 1/D_2(D_2-D_1)\beta_{j_1,0}$. Therefore P_1, P_2 are stable when $\beta_{j_1,0} > 0$ and $D_1 < D_2 < 0$.

$$J(P_2^{\pm}) = \begin{bmatrix} -2\beta_{j_1,0} & 0 \\ 0 & \frac{(D_2-D_1)}{D_2}\beta_{j_1,0} \end{bmatrix} \tag{83}$$

$$J(M^{\pm}) = \begin{bmatrix} \frac{-2D_2}{D_1+D_2}\beta_{j_1,0} & \frac{2D_1}{D_1+D_2}\beta_{j_1,0} \\ \frac{2D_1}{D_1+D_2}\beta_{j_1,0} & \frac{-2D_2}{D_1+D_2}\beta_{j_1,0} \end{bmatrix} \tag{84}$$

To analyze the stability of $M^{\pm}$, we find the trace and the determinant as follows.

$$\tau = \frac{-4D_2}{D_1+D_2}\beta_{j_1,0} \tag{85}$$

$$\Delta = \frac{4(D_2-D_1)\beta_{j_1,0}^2}{(D_1+D_2)} \tag{86}$$

Thus, $M^{\pm}$ is stable when $\tau < 0$ and $\Delta > 0$ and unstable otherwise. From Theorem 3 and from the trace and determinant of the Jacobian matrix of the truncated vector field, we can draw the following conclusions.

(1) The structure of the attractor depends on the signs of the parameters D_1, D_2 and on the sum $D_1 + D_2$. The signs of D_1, D_2 can either be negative or positive.
(2) The trace τ is negative when $D_1 + D_2 < 0$ and positive when $D_1 + D_2 > 0$ since for the existence of the steady states for the pure modes, we require $\beta_{10}D_2$ to be negative always.
(3) The determinant Δ is positive when both $D_2 - D_1$ and $D_2 + D_1$ have the same sign and negative when their signs alternates.

(4) Only cases (i) and (ii) under Theorem 3 are possible because each of cases (iii), (iv), and (v) leads to four steady states on the attractor which are all unstable.

5.1.4 | Transitions from a roll mode and a rectangular mode

In this case, $r = 2$, and the critical modes are as follows.

$$f_{11} = e_{j_1,j_2} = \cos\left(\frac{j_1 x}{L}\right)\cos(j_2 y),\ \ f_{20} = e_{2j_1 0} = \cos\left(\frac{2j_1 x}{L}\right)\ \ j_1, j_2 \in \mathbb{N}$$

$$\begin{pmatrix} u \\ v \end{pmatrix} = x_1(t)\begin{pmatrix} u_{j_1,j_2} \\ v_{j_1,j_2} \end{pmatrix} f_{11} + x_2(t)\begin{pmatrix} u_{2j_1,0} \\ v_{2j_1,0} \end{pmatrix} f_{20} + \begin{pmatrix} \Phi_u \\ \Phi_v \end{pmatrix} \tag{87}$$

$$\begin{pmatrix} \Phi_u \\ \Phi_v \end{pmatrix} = \Phi_{00}\begin{pmatrix} u_{0,0} \\ v_{0,0} \end{pmatrix} f_{00} + \Phi_{40}\begin{pmatrix} u_{4j_1,0} \\ v_{4j_1,0} \end{pmatrix} f_{40} + \Phi_{31}\begin{pmatrix} u_{3j_1,j_2} \\ v_{3j_1,j_2} \end{pmatrix} f_{3j_1,j_2} + \Phi_{22}\begin{pmatrix} u_{2j_1,2j_2} \\ v_{2j_1,2j_2} \end{pmatrix} f_{22} \tag{88}$$

$$\begin{aligned}
\Phi_{00}(x_1, x_2) &= q_{11}x_1^2 + q_{12}x_1x_2 + q_{22}x_2^2 \\
\Phi_{40}(x_1, x_2) &= h_{11}x_1^2 + h_{12}x_1x_2 + h_{22}x_2^2 \\
\Phi_{31}(x_1, x_2) &= m_{11}x_1^2 + m_{12}x_1x_2 + m_{22}x_2^2 \\
\Phi_{22}(x_1, x_2) &= n_{11}x_1^2 + n_{12}x_1x_2 + n_{22}x_2^2
\end{aligned}$$

By substituting the center part of the solution in (11), we obtain the following amplitude equations as in the previous cases

$$\begin{aligned}
\frac{dx_1}{dt} &= \beta x_1 + c\frac{\langle g_1, f_{11}\rangle}{\langle f_{11}, f_{11}\rangle} \\
\frac{dx_2}{dt} &= \beta x_2 + c\frac{\langle g_1, f_{20}\rangle}{\langle f_{20}, f_{20}\rangle}
\end{aligned} \tag{89}$$

such that at the critical crossing, we have let

$$\beta_{2j_1,0} = \beta_{j_1,j_2} = \beta.$$

Also, c is as defined in (32), and in this case, $g_1(u, v)$ is given below

$$g_1 = \phi_1(x_1^2 f_{11}^2 + 2x_1x_2f_{20}f_{11} + x_2^2 f_{20}^2) + \phi_2(x_1f_{11} + x_2f_{20})\Phi_u + \phi_3(x_1f_{11} + x_2f_{20})\Phi_v \quad . \tag{90}$$

In this case, the quadratic part of g_1 is given by

$$G_{21} = \phi_1(x_1^2 f_{11}^2 + 2x_1x_2f_{20}f_{11} + x_2^2 f_{20}^2). \tag{91}$$

Now we evaluate $\langle g_1, f_{20}\rangle$ and $\langle g_1, f_{11}\rangle$ as follows.

$$\begin{aligned}
\langle g_1, f_{11}\rangle &= \phi_1\rho_1 + \phi_2\rho_2 + \phi_3\rho_3 \\
\rho_1 &= \langle (x_1^2 f_{11}^2 + 2x_1x_2f_{20}f_{11} + x_2^2 f_{20}^2), f_{11}\rangle \\
\rho_2 &= \langle (x_1f_{11} + x_2f_{20})\Phi_u, f_{11}\rangle \\
\rho_3 &= \langle (x_1f_{11} + x_2f_{20})\Phi_v, f_{11}\rangle
\end{aligned} \tag{92}$$

Therefore,

$$\begin{aligned}\rho_1 &= \frac{L\pi^2}{4}x_1x_2\\ \rho_2 &= \frac{L\pi^2}{16}\left(4\Phi_{00}x_1+\Phi_{22}x_1+2\Phi_{31}x_2\right)\\ \rho_3 &= \frac{L\pi^2}{16}\left(4\Phi_{00}v_{00}x_1+\Phi_{22}v_{2j_1,2j_2}x_1+2\Phi_{31}x_2\right)\end{aligned}. \tag{93}$$

Similarly,

$$\begin{aligned}\langle g_1, f_{20}\rangle &= \phi_1\tilde{\rho}_1+\phi_2\tilde{\rho}_2+\phi_3\tilde{\rho}_3\\ \tilde{\rho}_1 &= \langle (x_1^2f_{11}^2+2x_1x_2f_{20}f_{11}+x_2^2f_{20}^2), f_{20}\rangle\\ \tilde{\rho}_2 &= \langle (x_1f_{11}+x_2f_{20})\Phi_u, f_{20}\rangle\\ \tilde{\rho}_3 &= \langle (x_1f_{11}+x_2f_{20})\Phi_v, f_{20}\rangle\end{aligned}. \tag{94}$$

Therefore,

$$\begin{aligned}\tilde{\rho}_1 &= \frac{L\pi^2}{8}x_1^2\\ \tilde{\rho}_2 &= \frac{L\pi^2}{8}\left(4\Phi_{00}x_2+\Phi_{31}x_1+2\Phi_{40}x_2\right)\\ \tilde{\rho}_3 &= \frac{L\pi^2}{8}\left(4\Phi_{00}v_{00}x_2+\Phi_{31}v_{3j_1,j_2}x_1+2\Phi_{40}v_{4j_1,0}x_2\right)\\ \langle f_{20}, f_{20}\rangle &= \frac{L\pi^2}{2}, \qquad \langle f_{11}, f_{11}\rangle = \frac{L\pi^2}{4}.\end{aligned} \tag{95}$$

Finally,

$$\begin{aligned}\langle g_1, f_{11}\rangle &= \frac{L\pi^2}{16}\left[4\phi_1x_1x_2+2\left(M_{00}+M_{31}\right)x_1x_2^2+\left(\frac{M_{22}}{4}+M_{00}\right)x_1^3\right]\\ \langle g_1, f_{20}\rangle &= \frac{L\pi^2}{8}\left[\phi_1x_1^2+\left(M_{00}+M_{31}\right)x_1^2x_2+(2M_{00}+M_{40})x_2^3\right]\end{aligned}. \tag{96}$$

Such that

$$\begin{aligned}\Phi_{40} &= \frac{V_{4j_1,0}}{2\beta_{4j_1,0}}x_2^2, \qquad \Phi_{31} = \frac{V_{3j_1,j_2}}{\beta_{3j_1,j_2}}x_1x_2\\ \Phi_{22} &= \frac{V_{2j_1,2j_2}}{4\beta_{2j_1,j_2}}x_1^2, \qquad \Phi_{00} = \frac{V_{0,0}}{4\beta_{0,0}}(x_1^2+2x_2^2)\end{aligned}. \tag{97}$$

Substituting (96) into (89), we obtain the reduced (amplitude) Equation (44).
We refer the interested reader to Şengül[16] for further detailed analysis on this case.

ACKNOWLEDGEMENT

The authors would like to thank the referee for his/her careful reading of this article and for his recommendations. There are no funders to report for this submission.

CONFLICT OF INTEREST

This work does not have any conflicts of interest.

ORCID

Umar Faruk Muntari https://orcid.org/0000-0001-7313-8025
Taylan Şengül https://orcid.org/0000-0003-4841-7326

REFERENCES

1. Ma T, Wang S. Introduction to dynamic transitions, dynamic transition theory. In: *Phase Transition Dynamics*. 2nd ed. Springer International Publishing; 2019:1-127. doi:10.1007/978-3-030-29260-7
2. Ma T, Wang S. Dynamic transition theory for thermohaline circulation. *Phys D: Nonlinear Phenom*. 2010;239(3-4):167-189. doi:10.1016/j.physd.2009.10.014
3. Ma T, Wang S. Dynamic transition and pattern formation for chemotactic systems. *Discrete Contin Dyn Syst - B*. 2014;19(9):2809-2835. doi:10.3934/dcdsb.2014.19.2809
4. Jia L, Li L. Stability and dynamic transition of vegetation model for flat arid terrains. *Discrete Contin Dyn Syst - B*. 2021. doi:10.3934/dcdsb.2021189
5. Sekisaka A, Yamamoto H. Instability in the nebula model of compressive viscous gases. *Phys D: Nonlinear Phenom*. 2020;403:132290. doi:10.1016/j.physd.2019.132290
6. Pan Z, Kieu C, Wang Q. Hopf bifurcations and transitions of two-dimensional quasi-geostrophic flows. *Communications on Pure & Applied Analysis*. 2021;20(4):1385-1412. doi:10.3934/cpaa.2021025
7. Lu C, Mao Y, Wang Q, Yan D. Hopf bifurcation and transition of three-dimensional wind-driven ocean circulation problem. *J Differ Equ*. 2019;267(4):2560-2593. doi:10.1016/j.jde.2019.03.021
8. Ma T, Wang S. Phase Transitions for the Brusselator Model. *J Math Phys*. 2011;52(3):033501. doi:10.1063/1.3559120
9. Tzou JC, Matkowsky BJ, Volpert VA. Interaction of Turing and Hopf modes in the superdiffusive Brusselator model. *Appl Math Lett*. 2009;22(9):1432-1437.
10. Guo B, Han Y. Attractor and spatial chaos for the Brusselator in RN. *Nonlinear Anal: Theory, Methods Appl*. 2009;70(11):3917-3931.
11. Prigogine I, Lefever R. Symmetry breaking instabilities in dissipative systems. II. *J Chem Phys*. 1968;48(4):1695-1700.
12. Rech PC. Multistability in a Periodically Forced Brusselator. *Braz J Phys*. 2021;51(1):144-147. doi:10.1007/s13538-020-00806-2
13. Seara DS, Machta BB, Murrell MP. Irreversibility in dynamical phases and transitions. *Nat Commun*. 2021;12(1):392. doi:10.1038/s41467-020-20281-2
14. Llibre J, Valls C. Global qualitative dynamics of the Brusselator system. *Math Comput Simul*. 2020;170:107-114.
15. Murray JD. *Mathematical Biology II: Spatial Models and Biomedical Applications*, 3rd ed. Interdisciplinary Applied Mathematics, Mathematical Biology. New York: Springer-Verlag; 2003. doi:10.1007/b98869
16. engül T. Dynamical transition theory of hexagonal pattern formations. *Commun Nonlinear Sci Numer Simul*. 2020;91:105455. doi:10.1016/j.cnsns.2020.105455
17. Choi Y, Ha T, Han J, Kim S, Lee DS. Turing instability and dynamic phase transition for the Brusselator model with multiple critical eigenvalues. *Discrete Contin Dyn Syst*. 2021;41(9):4255. doi:10.3934/dcds.2021035
18. Sengul T, Shen J, Wang S. Pattern formations of 2D Rayleigh-Bénard convection with no-slip boundary conditions for the velocity at the critical length scales. *Math Methods Appl Sci*. 2015;38(17):3792-3806. doi:10.1002/mma.3317

How to cite this article: Muntari UF, Şengül T. Dynamic transitions and Turing patterns of the Brusselator model. *Math Meth Appl Sci*. 2022;45(16):9130-9151. doi:10.1002/mma.8296